Journal of Power Sources 195 (2010) 2644–2648

Contents lists available at ScienceDirect

Journal of Power Sources

journal homepage: www.elsevier.com/locate/jpowsour

Short communication

Fabrication and evaluation of anode and thin Y_2O_3-stabilized ZrO_2 film by co-tape casting and co-firing technique

Shiru Le[a,b], Ke Ning Sun[a,*], Naiqing Zhang[a], Xiaodong Zhu[a,b], Hanxiao Sun[a], Yi Xing Yuan[b], Xiaoliang Zhou[a]

[a] Natural Science Research Center, Academy of Fundamental and Interdisciplinary Sciences, Harbin Institute of Technology, No. 92, XiDazhi Street, Harbin, Heilongjiang Province 150001, PR China
[b] Postdoctoral Research Center for Civil Engineering(Municipal Engineering),School of Municipal and Environmental Engineering, Harbin, Heilongjiang Province, PR China

ARTICLE INFO

Article history:
Received 19 October 2009
Received in revised form 9 November 2009
Accepted 9 November 2009
Available online 14 November 2009

Keywords:
Solid oxide fuel cell
Co-tape casting
Co-firing
Large size
Anode

ABSTRACT

Co-tape casting and co-firing of supporting electrode and electrolyte layers could drastically increase productivity and reduce fabrication cost. In this study, Ni-YSZ anode supporting electrode and the YSZ electrolyte with the size of 6.5 cm × 6.5 cm have been successfully fabricated by co-tape casting and co-firing technique. The cell with 1.5 mm anode and 10 μm electrolyte is flat without warping, cracks or delaminations. The power density reaches 661, 856, 1085 mW cm^{-2} at 0.7 V and 750, 800 and 850 °C, respectively. The EIS results demonstrate that the cathodic electrochemical resistance is 0.0680 Ω cm^2, about twice of the anode's which is 0.0359 Ω cm^2. SEM images show the dense YSZ film had a crack free of surface morphology. The anode and cathode layers are well-adhered to the YSZ electrolyte layer. The $La_{0.8}Sr_{0.2}MnO_{3-\delta}$ particles do not form a continuous network. Optimization of finer cathodic microstructure and anodic porosity are underway.

1. Introduction

A solid oxide fuel cell (SOFC) is an electrochemical energy converter with high efficiency and low emission of pollutants [1,2]. A traditional SOFC is generally composed of three components: the electrolyte (8 mol% Y_2O_3-stabilized ZrO_2, YSZ), the anode (Ni-YSZ composite cermet) and the cathode (lanthanum manganite based cathode, $La_{0.8}Sr_{0.2}MnO_{3-\delta}$, LSM). However the SOFC still faces a number of challenges that hinder its commercialization, among which are the system reliability and the fabrication cost as well as the major issues in its practical application as a power generator [3]. Therefore, most researches on SOFC are mainly focused on the developments of commercially available SOFC technology with superior electrochemical performance [4,5].

Several methods for preparing SOFC electrolyte have been investigated: electrochemical vapor deposition (EVD) [6], chemical vapor deposition (CVD) [7], sol–gel processing [8], spray pyrolysis [9], physical vapor deposition [10], pulsed laser deposition [11], screen printing [12], tape casting [13], coat-mix [14], cold pressing [15] and other methods. However, these methods are relatively costly or involve several steps to fabricate the anode and electrolyte together. The replacement of expensive and complex processing steps for anode-supported electrolyte film by cheaper, simpler, and continuous techniques has to be considered.

Conventional SOFC fabrication involves multiple sintering steps. Therefore, the manufacturing costs of SOFCs could be lowered by employing a single-step co-firing technique. A promising design is the simultaneous fabrication of electrolyte and supporting anode [16], and then co-fired together. This could increase productivity and reduce fabrication cost.

Tape casting is a well-known cost-effective technique to produce large area, thin and flat ceramic tapes. However, this method has not been extensively employed in the fabrication of co-tape casting the electrolyte and its supporting anode electrode, because it is difficult to obtain both a thin electrolyte layer with no gas permeability and co-firing button cells without processing defects [17].

In this study, thin YSZ electrolyte and supporting anode have been successfully fabricated by co-tape casting and co-firing technique. The resulting cell is flat without warping, cracks or delaminations. This could be cost-effective when applied to mass production. The open current voltage of the cell is 1.13 V at 800 °C, which nearly reaches the theoretical value, with electrolyte at about 10 μm in thickness. The power density of the cell is 856 mW cm^{-2} at 0.7 V and 800 °C.

* Corresponding author. Tel.: +86 451 86412153; fax: +86 451 86412153.
E-mail address: leshiru2005@yahoo.com.cn (K.N. Sun).

0378-7753/$ – see front matter © 2009 Elsevier B.V. All rights reserved.
doi:10.1016/j.jpowsour.2009.11.039

Table 1
Slurry composition for tape casting anode and YSZ electrolyte.

	Function	Composition	
		Electrolyte	Anode
YSZ (g)	Ceramic powder	100	45
NiO (g)	Ceramic powder	0	55
Ethyl alcohol (mL)	Solvent	150	37.5
Butanone (mL)	Solvent	60	37.5
Triethanolamine (mL)	Dispersant	0.5	2.0
Diethyl-o-phthalate (DEP)	Plasticizer	2.5	9.35
Polyvinyl butyral (PVB, g)	Plasticizer	12	11.4
Polyethylene glycol (PEG, g)	Binder	6.9	12.15
Starch (g)	Pore former	0	15

2. Experimental

2.1. Tape casting process

The slurry compositions for tape casting were shown in Table 1. Electrolyte thin film and anode were prepared by co-tape casting. The slurries for tape casting process were prepared as the following. In the first step, the YSZ (TZ8Y, Tosoh, Japan) for electrolyte, the NiO (Inco, USA) and the YSZ for anode were homogenized in a planetary mill for 24 h, with dispersant in a mixture of butanone and ethyl alcohol (EtoH) as solvent. Secondly, the polyvinyl butyral (PVB) as binder, the diethyl-o-phthalate (DEP), and a mixture of polyethylene glycol (PEG) as plasticizer, were added, respectively, then milled for another 24 h. Prior to tape casting, the slurries were vacuum pumped for about 30 min in order to remove air. The YSZ film was first cast onto the plate and allowed to dry in air for minutes, then followed by the anode layer on the top. After drying overnight at room temperature, the multilayer green tapes were detached and co-fired at 1400 °C for 5 h in one sintering step. The cathode paste of $La_{0.8}Sr_{0.2}MnO_3$-δ-YSZ was screen-printed on the YSZ electrolyte surface and sintered at 1150 °C for 2 h.

2.2. Characterizations

The linear shrinkages of the Ni-YSZ anode and YSZ electrolyte green tapes were studied using a NETZSCH DIL 402PC dilatometer in air at a heating rate of 0.5 °C min^{-1} to 1400 °C, then decreased to 25 °C at a cooling rate of 0.5 °C min^{-1}. The *I–V* and *I–P* tests were demonstrated in details elsewhere [18]. The discharging performance of cells was measured by Arbin Instruments, using H_2 with 3% H_2O as fuel at a flow rate of 100 sccm and air as oxidant. The electrochemical impedance spectroscopy was made with Princeton Applied PARSTAT 2273 impedance analyzer under open circuit condition for the frequency range of 0.05 Hz to 100 kHz. Scanning electron microscopy (SEM) was used to observe the microstructures with a Hitachi S4700. The porosity was measured by Archimedes method and KEITHLEY 2400 sources meter was used to detect the electronic conductivity.

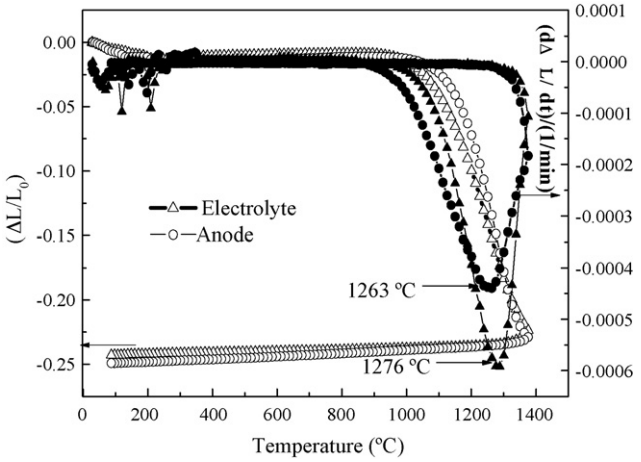

Fig. 1. Dilatometric curves of anode and electrolyte green tape measured in air.

3. Results and discussions

The shrinkage mismatch during sintering will induce large residual stresses in the cell, and this may induce micro-cracks or a delamination between the electrolyte and the anode. These damages decrease the cell performance, and sometimes cause destruction. Fig. 1 presents the dilatometric traces of Ni-YSZ anode and YSZ electrolyte green tapes at a heating rate of 0.5 °C min^{-1} to 1400 °C, then to 25 °C at the same rate. Most shrinkages occurred during the heating stage, which demonstrated that the residual stresses of the cell induced during the heating stage, but not the cooling stage. The temperature of maximum shrinkage rate of Ni-YSZ anode green tape was 1276 °C, which was contiguous to 1263 °C for that of YSZ green tape. This reduced the residual stresses in the

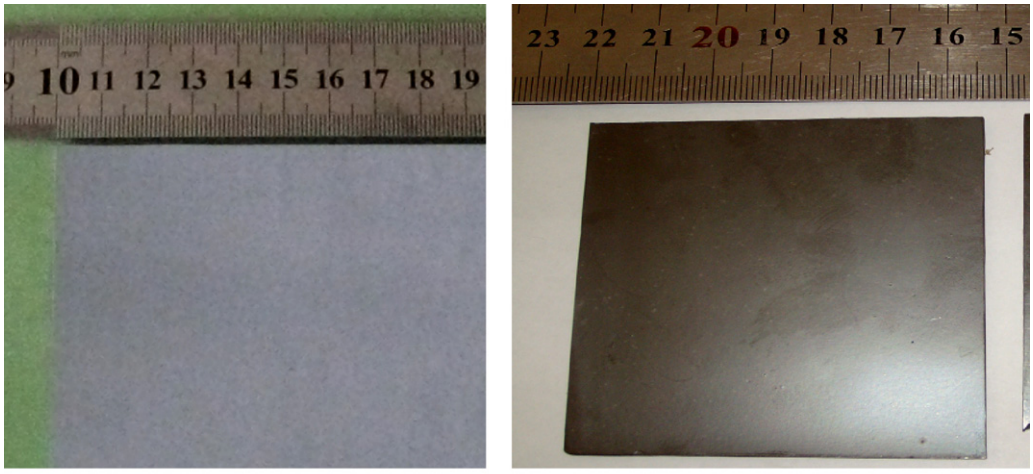

Fig. 2. Photographic images anode-supported electrolyte: (a) green tape and (b) after co-firing.

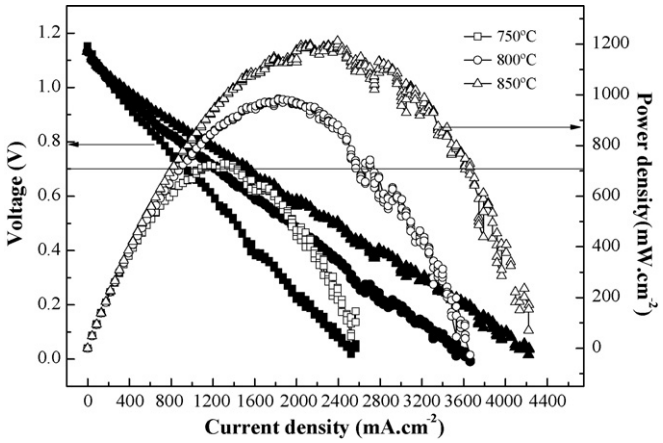

Fig. 3. *I–V* and *I–P* curves of a unit cell.

cell. The linear shrinkages of Ni-YSZ anode green tape and YSZ electrolyte green tape was 24.6% and 24.9%, respectively. There was only 0.3% mismatch for these two green tapes. The similar shrinkage values promised the feasibility of the co-firing process with the slurry compositions in this study.

As demonstrated in Fig. 2, the YSZ thin film and supporting anode green tapes were successfully fabricated by co-tape casting technique. The green tape was 8.6 cm × 8.6 cm. After co-firing at 1400 °C for 5 h, a size of 6.5 cm × 6.5 cm Ni-YSZ anode-supported YSZ thin electrolyte film was successfully fabricated. The cell was flat without processing defects such as warping, delaminations, and cracks. The porosity of the cell was 39.5%. The conductivity of the anode electrode was 2.0×10^3 S cm^{-1} after reducing in hydrogen atmosphere at 800 °C.

To property evaluate the properties of the obtained anode-supported thin YSZ film, a small button cell with 20 mm in diameter was measured. Fig. 3 shows the typical *I–V* and *I–P* curves of the button cell consisting of Ni-YSZ anode, YSZ thin electrolyte film and LSM cathode, measured at temperature between 750 °C and 850 °C. The open circuit voltages (OCVs) registered were 1.15, 1.13, and 1.13 V at 750, 800 and 850 °C, respectively, which were in good agreement with the theoretical values calculated from the Nernst equation. The high open circuit voltages close to the theory values indicated dense YSZ electrolyte film free of voids, pinholes or cracks. The leakage of the fuel gas was negligible for the cell. The power density reached 661, 856, 1085 mW cm^{-2} at 0.7 V and 750, 800 and 850 °C, respectively. This was higher than those prepared

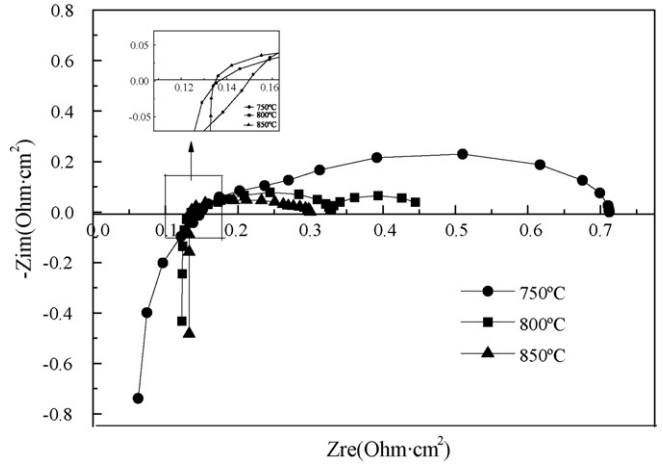

Fig. 4. Impedance spectra of the unit cells at different temperatures.

Table 2
Electrochemical characteristics of the cell at different temperatures and comparison with other researchers' results.

Temperature	R_s (Ω cm^2)	R_p (Ω cm^2)	R_p (Ω cm^2, references)
750	0.152	0.560	0.90 [16]
800	0.135	0.310	1.0 [18]
850	0.135	0.265	

by co-tape casting Ni-YSZ anode and YSZ electrolyte, respectively, then laminated together, with 160 mW cm^{-2} at 0.7 V and 750 °C [19], co-tape casting of LSM/SSZ cathode supported YSZ electrolyte, 420 mW cm^{-2} at 0.7 V and 800 °C [20].

To examine the resistance of the electrolyte and the polarization resistances of the electrodes in more detail, the electrochemical impedance tests were conducted under the open circuit condition. Fig. 4 presents the impedance spectra of the button cell (NiO-YSZ/YSZ/LSM) measured under open circuit conditions from 750 to 850 °C. The solid lines in Fig. 4 were the fitted results of the ZsimpWin program.

The high frequency intercepts with the real axis represents the ohmic resistances of the cell (R_s), involving ionic resistance of the electrolyte, and some contact resistance associated with interfaces. The difference between the high frequency and low frequency intercepts represents the polarization resistance (R_p), including cathodic and anodic electrochemical polarization, cathodic and anodic gas diffusion polarization. The values of the symbols were illustrated in Table 2. The R_s increased from 0.135 Ω cm^2 at 850 °C to 0.152 Ω cm^2 at 750 °C. The R_p increased from 0.265 Ω cm^2 at 850 °C to 0.560 Ω cm^2 at 750 °C. R_p was larger than R_s, indicating that polarization resistances appeared to be more dominant.

For anode-supported thin YSZ film, arc 1 and arc 2 of the electrochemical impedances are used to describe the cathodic and anodic electrochemical polarization losses, respectively. Arc 3 and arc 4 are used to describe gas diffusion and conversion in the cathode and anode, respectively [21]. These arcs were fitted in Fig. 5. The dotted lines were the fittings from the equivalent circuit model. Table 3 summarizes the correspondence between the arcs and their components in the equivalent circuit.

Table 3 indicates that the gas diffusion resistance in the anode electrode was 0.0669 Ω cm^2, about twice of 0.0359 Ω cm^2 of the cathode's. The model shown by Chan [22] demonstrated that the effect of concentration polarization in the anode is much greater

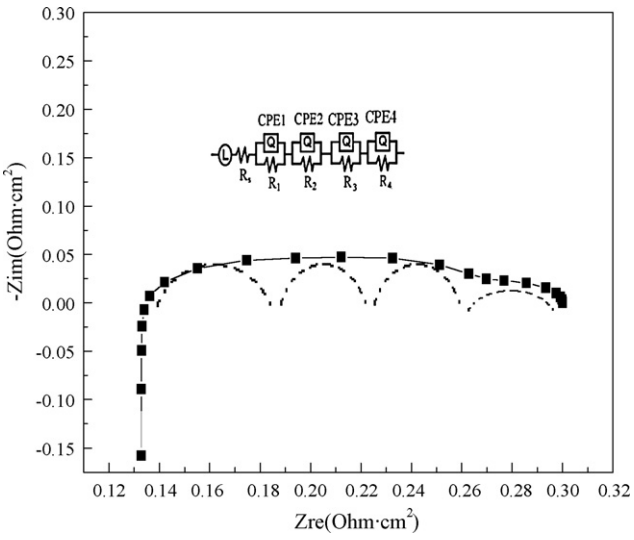

Fig. 5. Impedance spectra of the unit cells at 850 °C. Measured date (symbols), fitted spectrum (full line), and fitted spectrum depicted as individuals arc dotted line.

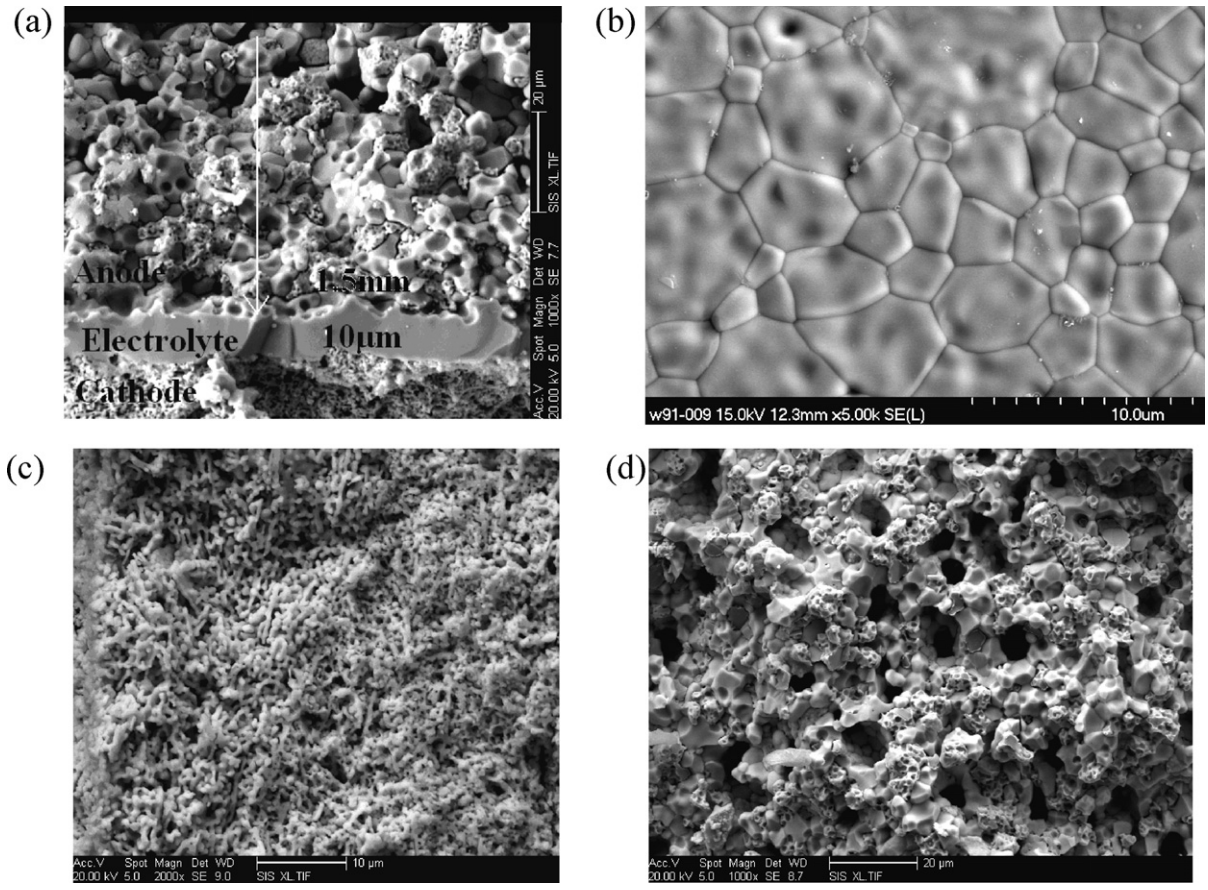

Fig. 6. SEM images of the button cell (a) cross-section of the button cell, (b) surface image of the electrolyte, (c) cathode, and (d) anode.

than that in the cathode of an anode-supported cell. This is consistent with the results of Suzuki et al. [23]. Thus, providing sufficient porosity of the anode could lead to improvement of the cell performance. However, the anodic electrochemical resistance was only $0.0310\,\Omega\,cm^2$, about half of $0.0680\,\Omega\,cm^2$ of cathode electrode's, demonstrating that finer cathodic microstructure should be examined more closely in future research.

The cross-sectional SEM images of the co-firing cell were shown in Fig. 6. The YSZ electrolyte with 10 μm thickness supported by the anode electrode with 1.5 mm in thickness. The YSZ film was essentially dense, with no open pinholes. The uniform and clear grains with a size of 2–5 μm were obtained. The YSZ film had a continuous and crack free surface morphology. Both the anode and cathode layer were well-adhered to the YSZ electrolyte layer. The pores in the anode were not uniformly distributed, providing insufficient gas flow channels, leading to high anodic gas diffusion polarization. The distribution of the LSM particles appeared to be discrete and did not form a continuous network, leading to high cathode electrochemical polarization. The cathode electrode with cathode functional layer and current collector layer, with continuous LSM particle will improve its performance [24]. Optimization of finer cathodic microstructure should be investigated in future. The evaluation of the cell in an SOFC stack is underway.

Table 3
Arcs that characterized losses of a full cell.

Arcs	$R\,(\Omega\,cm^2)$	Characteristics
Arc 1	0.0680	Cathode polarization
Arc 2	0.0310	Anode polarization
Arc 3	0.0359	Cathode diffusion
Arc 4	0.0669	Anode diffusion

4. Conclusions

Ni-YSZ anode-supported YSZ electrolyte with the size of 6.5 cm × 6.5 cm have been successfully fabricated by co-tape casting and co-firing technique. The cell was flat without warping, cracks or delaminations. This could significantly increase productivity and reduce fabrication cost. The OCVs of the cell were close to the theoretical values. The power density of a button cell reached 661, 856, 1085 mW cm^{-2} at 0.7 V and 750, 800 and 850 °C, respectively. Further research should be focused on finer cathodic electrochemical polarization and higher anodic porosity. Evaluation of SOFC cell in a stack is currently underway.

Acknowledgements

This work was Project Supported by Development Program for Outstanding Young Teachers in Harbin Institute of Technology with Number HITQNJS.2008.059. Heilongjiang Posterdocteral Research (LBH-Z08163), China Postdoctoral Science Foundation (no. 20080430134 and 200902384) and Natural Scientific Research Innovation Foundation in Harbin Institute of Technology (no. HIT.NSRIF.2008.22).

References

[1] Z.-P. Shao, M.H. Sossina, Nature 431 (2004) 170–173.
[2] Y.-H. Huang, R.I. Dass, Z.-L. Xing, et al., Science 312 (2006) 254–257.
[3] Q.L. Liu, S.H. Chan, C.J. Fu, et al., Electrochemistry Communications 11 (2009) 871–874.
[4] S. Menzer, G. Coors, D. Beeaff, et al., Proceedings of the 6th International Conference on Fuel Cell Science Engineering and Technology, 2008, pp. 33–38.

[5] P. Timakul, S. Jinawath, P. Aungkavattana, Ceramics International 34 (2008) 867–871.
[6] Z.-T. Wu, X.-L. Dong, W.-Q. Jin, et al., Journal of Membrane Science 291 (2007) 172–179.
[7] S. Preusser, U. Stimming, K. Wippermann, Electrochimica Acta 39 (1994) 1273–1289.
[8] C. Suciu, A.C. Hoffmann, A. Vik, F. Goga, Chemical Engineering Journal 138 (2008) 608–615.
[9] M.F. García-Sánchez, J. Peña, A.G. Ortiz, et al., Solid State Ionics 179 (2008) 243–249.
[10] D. Beckel, A. Bieberle-Hütter, A. Harvey, et al., Journal of Power Sources 173 (2007) 325–345.
[11] J.W. Yan, H. Matsumoto, T. Akbay, T. Yamada, T. Ishihara, Journal of Power Sources 157 (2006) 714–719.
[12] X.-D. Ge, X.-Q. Huang, Y.-H. Zhang, et al., Journal of Power Sources 159 (2006) 1048–1050.
[13] H. Moon, S.D. Kim, S.H. Hyun, et al., International Journal of Hydrogen Energy 33 (2008) 1758–1768.
[14] D. Simwonis, H. Thülen, F.J. Dias, A. Naoumidis, et al., Journal of Materials Processing Technology 92–93 (1999) 107–111.
[15] X.-H. Fang, G.-Y. Zhu, C.-R. Xia, et al., Solid State Ionics 168 (2004) 31–36.
[16] P. Timakul, S. Jinawath, P. Aungkavattana, Materials Science and Engineering A 420 (2006) 171–175.
[17] A. Sanson, P. Pinasco, E. Roncari, Journal of the European Ceramic Society 28 (2008) 1221–1226.
[18] J.-R. Kong, K.-N. Sun, D.-R. Zhou, et al., Journal of Power Sources 166 (2007) 337–342.
[19] J.-H. Song, S.-I. Park, Jong-Ho, et al., Journal of Materials Processing Technology 198 (2008) 414–418.
[20] C. Zhao, R. Liu, S. Wang, et al., Electrochemistry Communications 11 (2009) 842–845.
[21] R. Barfod, M. Mogensen, T. Klemenso, et al., Journal of the Electrochemical Society 154 (2007) B371–B378.
[22] S.H. Chan, K.A. Khor, Z.T. Xia, Journal of Power Sources 93 (2001) 130–140.
[23] T. Suzuki, Z. Hasan, Y. Funahashi, et al., Science 325 (2009) 852–855.
[24] V.A.C. Haanappel, J. Mertens, D. Rutenbeck, et al., Solid State Ionics 141 (2005) 216–226.